From Z-Machines to ALMA: (Sub)millimeter Spectroscopy of Galaxies
ASP Conference Series, Vol. TBD, 2006
A. J. Baker, J. Glenn, A. I. Harris, J. G. Mangum, and M. S. Yun, eds.

The Zpectrometer: an ultrawideband spectrometer for the GBT

A.I. Harris[1], A.J. Baker[1,2], P.R. Jewell[2], K.P. Rauch[1], S.G. Zonak[1], K. O'Neil[2], A.L. Shelton[2], R.D. Norrod[2], J. Ray,[2] and G. Watts[2]

[1]*Department of Astronomy, University of Maryland, College Park, MD 20742;* [2]*National Radio Astronomy Observatory, P.O. Box 2, Green Bank, WV, 24944*

Abstract. We describe the *Zpectrometer*, an ultra-wideband radio spectrometer for the Green Bank Telescope (GBT). Observations with this instrument will be important in understanding the star formation, metal production, and structure formation histories of the Universe. The *Zpectrometer* covers the full 13.5 GHz-wide Ka-band with a set of analog lag correlation spectrometers in a multi-channel correlation radiometer architecture. Its bandwidth and stability, combined with the GBT's collecting area, enable sensitive and efficient spectral searches for molecules in high redshift galaxies. The instrument is optimized for observations of low-excitation spectral lines from the carbon monoxide (CO) molecule at redshifts of $1.88 \leq z \leq 3.43$ and $4.76 \leq z \leq 7.87$.

All high-redshift radio molecular detections to date have started from optical redshifts. *Zpectrometer*'s wide bandwidth bypasses this selection effect and enables it to detect new classes of sources. In addition to finding precise redshifts, its spectra with velocity resolution of approximately 150 km s^{-1} probe kinematical signs of interaction and derive dynamical mass estimates. Both cold and warm gas emit low-J lines, and these observations are critical constraints on radiative transfer models of physical conditions.

1. Introduction

The *Zpectrometer*'s main purpose is to study star and galaxy formation in the early Universe. The histories of these processes are coupled with the evolution of large-scale structure and the formation of metals, and are thus of fundamental cosmological interest. The *Zpectrometer* is a heterodyne spectrometer that will cover the entire Ka-band (26.5-40 GHz) at the 100-meter Robert C. Byrd Green Bank Telescope (GBT). This ultrawideband spectrometer is a spectral bridge between observations with continuum cameras that search for luminous dusty galaxies at high redshift and line observations with radio and millimeter-wave interferometers. It is optimized for velocity-resolved spectroscopy of cold and warm molecular gas to explore the physical state and mass of young massive galaxies. Line-resolved spectroscopy will also constrain the dynamical state of the gas for mass estimates and find the spectral signatures of interactions.

Of the instruments described this *Proceedings*, the *Zpectrometer* covers the lowest frequencies, corresponding to rest-frame millimeter-wave spectral lines from low-excitation molecular transitions. With nearly 1000 spectral channels across the band, its spectral resolution is sufficient to characterize bulk motions

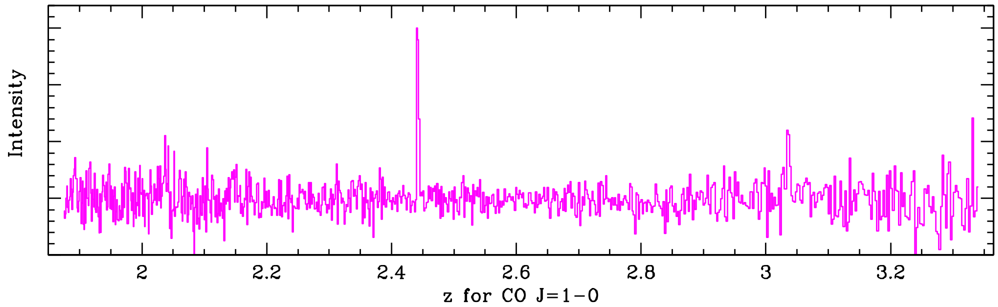

Figure 1. Simulated *Zpectrometer* spectrum: the full Ka-band in 825 channels with CO $J = 1$–0 lines at $z = 2.34$ (34.5 GHz) and 3.03 (28.5 GHz). The noise in the simulation is scaled by the GBT's measured receiver temperature and telescope aperture efficiency.

in the gas to quantify rotational speeds within galaxies, find nuclear rings, and search for evidence of interaction.

By covering the entire Ka-band, the *Zpectrometer* is able to make velocity-unbiased searches for low excitation spectral lines of carbon monoxide (CO) molecules to determine precise redshifts of young galaxies at cosmological distances. Figure 1 is a simulated *Zpectrometer* spectrum over its full CO $J = 1$–0 $1.88 \leq z \leq 3.43$ (lookback times of 10.1–11.8 Gyr) band with a spectral resolution of approximately 150 km s^{-1}. The same observed-frame frequencies also correspond to the $J = 2$–1 transition at $4.76 \leq z \leq 7.87$ (from 12.4–13.0 Gyr ago, just 700 Myr after the Big Bang), covering the era of final reionization.

A combination of HEMT amplifier receivers and wideband analog lag spectrometers makes it possible to search the Ka-band's entire 41% fractional bandwidth (instantaneous bandwidth divided by average frequency) for spectral lines. A correlation radiometer architecture, similar to the continuum radiometers on the WMAP satellite, will help provide excellent baseline stability.

The GBT is uniquely well suited to studies of the early Universe. It has an off-axis reflector with an unblocked 100-meter equivalent aperture and a large receiver cabin at the secondary focus. The GBT's active surface already provides excellent performance in the Ka-band, and the surface will improve as upgrades continue for telescope operation at 115 GHz. This combination of geometrical area and a precise surface gives the GBT an enormous collecting area; at centimeter wavelengths the GBT's combination of geometrical area and precise surface gives it an effective collecting area larger than the 27-antenna Expanded Very Large Array, EVLA. Combined with state-of-the-art receivers, the GBT provides extraordinary sensitivity for observations of point sources.

2. Star and galaxy formation in the early Universe

Other papers in this *Proceedings* discuss observational evidence that the cosmic star formation rate peaked somewhere between z of 2 and 5. Current wisdom holds that $z \sim 2$–3 defines the epoch when many of the long-lived stars in the Universe formed, the assembly of massive galaxies by mergers was especially vigorous, super-massive black holes formed, and QSO activity increased dramat-

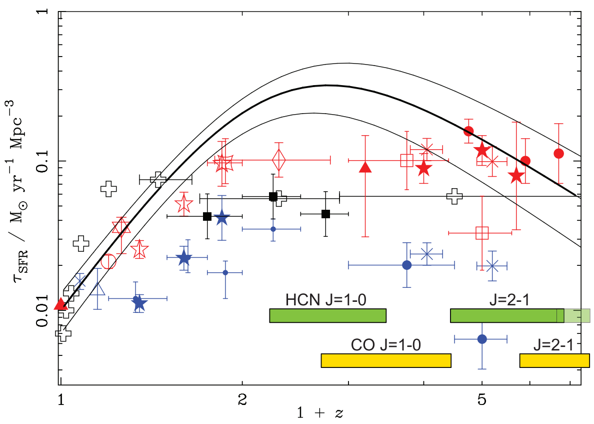

Figure 2. Star formation rate density versus redshift z, updated from Blain et al. 2002 (Blain 2004, priv. comm.). Points with error bars are derived from rest-frame UV observations and show the considerable uncertainty in the star formation rate density. The heavy solid line is the best-fit evolutionary model derived from submillimeter and far-IR observations alone; lighter lines show model error limits. Bars toward the bottom of the panel show Ka-band coverage for low-J CO and HCN lines.

ically. The details of this picture are far from settled, however. An important constraint on theoretical mass-assembly models is galactic mass as a function of redshift. Rest-frame millimeter-wave molecular emission escapes easily through the dust that hides young massive galaxies in optical images, with velocity-resolved spectroscopy providing dynamical mass estimates independent of the uncertainties in dust or molecular emissivity per unit mass.

Although of order 30 galaxies and quasars have been detected in CO at redshifts $1.4 < z < 6.4$ (summaries in (e.g. Hainline et al. 2004; Greve et al. 2005; Genzel 2004), it is important to recognize that *all of the molecular detections to date have started from optical redshifts*. The need for optical detection complicates and biases searching for and exploring the state of molecular gas in young galaxies. Initial *Zpectrometer* molecular line observations will have fewer and different selection effects: it will make an unbiased search for molecular emission over a very wide band.

An obvious search strategy for the dusty submillimeter galaxies (SMGs) is to start with source positions from the many sensitive sub-mm and mm-wave continuum cameras that have been built to observe the high-z universe. All of the ground-based cameras provide source position accuracies well matched to the GBT's 23″–15″ Ka-band beam, eliminating the need to search within the continuum camera beams.

The *Zpectrometer* will also sample populations other than the dusty galaxies selected in the submillimeter. Work of this kind is important for exploring the connections between the dusty galaxies and other populations. It will be sensitive to galaxies with warmer dust that the Spitzer Space Telescope (SST) detects but that 850 μm continuum observations miss (e.g. Houck et al. 2005; Yan et al. 2005). More targets will emerge from other far-IR through X-ray deep imaging (e.g. Herschel-SPIRE, Chandra, Newton-XMM...) and steep-spectrum radio galaxy searches Reuland et al. (e.g. 2004).

2.1. Lines

Although the *Zpectrometer*'s band is very wide, the 115 GHz spacing between CO transitions is too large for more than one line to appear in the the band until $z \sim 10$. Emission from the HCN molecule, a tracer of dense gas associated with star formation (Gao and Solomon 2004), will be detectable from bright sources and will provide redshift confirmation over the redshift ranges $z = 1.88$–2.41 where the CO and HCN $J = 1$–0 lines both fall in the band (Fig. 2).

Millimeter-wave interferometers will quickly follow most or all of the *Zpectrometer* detections with observations of higher-J CO lines. This will provide unambiguous redshifts from detection of two or more lines, constrain physical conditions with line ratios, and generate detailed spatial maps and spectra. High-resolution spectral imaging is necessary to identify sources that are gravitationally lensed and to build models for the gravitational magnification. Interferometers have relatively narrow bandwidths at present and must start with precise redshifts. Shifts between optical and radio lines can be large in radio galaxies and may be the reason than at least some of the narrowband CO searches in dusty galaxies based on optical redshifts have failed. If insufficient bandwidth has caused the nondetections, *Zpectrometer* observations will enable new high-resolution observations of the early Universe.

2.2. Cold gas and low-J lines

Observations in the Ka-band contain the lowest-excitation transitions of the abundant carbon monoxide molecule. Lines from low-J states probe relatively cold or low density gas as well as the warm and dense gas that rest-frame submillimeter emission preferentially traces. CO $J = 1$–0 luminosity is therefore taken as a proxy for molecular gas mass in disk galaxies and ULIRGs (Downes and Solomon 1998). Almost all of the high-z CO detections to date have been at millimeter wavelengths because of the lack of suitable cm-wave instrumentation.

Measurements of the low excitation lines are necessary for modeling the realistic situation of a source with more than one temperature component. Figure 3 is a two-component decomposition of a $z = 3$ starburst based on the conditions in the starburst galaxy M82. Constraining the relative amounts of cold and warm gas requires low-J measurements sensitive to cool gas; without this information, the properties of even the warm gas component alone are uncertain within orders of magnitude. Flux plots underemphasize the mass in a cool component because of the frequency squared scaling between brightness temperature and flux, so full modeling is needed to understand the amount of gas in each component.

If the relatively nearby universe is any guide – and it may not be – a cold molecular gas component will be more extended than the small highly excited regions that contain gas emitting in the mid-J rotational transitions. In the local universe, observations of the CO $J = 6$–5 and 7–6 lines from starburst galaxies show that the submillimeter emission is strongly concentrated in nuclei (Bradford et al. 2003; Ward et al. 2003; Mao et al. 2000; Harris et al. 1991) and is associated with the strong UV or cosmic ray fluxes from young massive

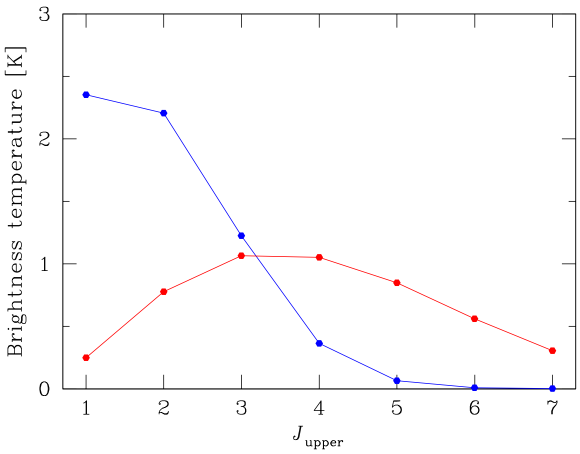

Figure 3. Two-component radiative transfer model of a $z = 3$ starburst nuclei patterned on conditions in M82. A 23 K component has peak emission at low rotational quantum numbers J, while a 208 K component is optically thin in the low-J transitions and peaks near $J \sim 3$–4. Both components in this model have equal mass.

stars. Luhman et al. (2003) compare ISO 158 μm [C II] and CO $J = 1$–0 emission, finding that the filling factor of CO can be up to an order of magnitude larger than PDR-tracing [C II] in ULIRGs, although the scales are similar in normal and starburst galaxies. In absolute terms, CO $J = 1$–0 observations of Arp 220, Arp 299, Mrk 231, and other luminous galaxies (Scoville et al. 1997; Downes and Solomon 1998) show that much of the low-J CO emission comes from extended components with larger sizes and filling factors than the infrared-luminous nuclei. For high-redshift objects, observation of the intensity and lineshape of cold gas is necessary to reveal the relative amounts of cool extended and warm compact emission by finding filling factors as part of radiative transfer modeling.

2.3. Typical integration times

Extrapolating from detections of the current sample of dusty galaxies and quasars provides estimates for interesting line fluxes and integration times. Many of these sources have mm-wave line fluxes of a few mJy. With a representative set of telescope parameters and source zenith angles we derive a system temperature of 100 K and an rms fluctuation of 0.18 mK after 10 hours of integration in a single 17 MHz channel. With the GBT's conversion of 1.1 K/Jy (350 μm rms surface, 33 GHz), this corresponds to 0.16 mJy rms. This integration time is feasible for some tens of sources per year. Line flux increases with frequency for a thermalized source, and cosmological dimming is small at high redshift, so observations of higher-J lines is quite possible at even higher redshifts.

3. Technical aspects

3.1. Correlation radiometry

A key element of the *Zpectrometer* is its use of correlation techniques in the receiving system. Cross-correlating brings the stability advantages of a continuum correlation radiometer to spectroscopy. Spectroscopy with correlation techniques on a single-dish telescope is unusual in radio astronomy. A number of groups investigated single-dish correlation receivers during the 1960s as an alternative to the standard Dicke-switched radiometer, but the cost of building two receiver chains and cross-correlators limited their use to special cases such as centimeter-wave radio continuum studies, a rapid-response millimeter-wave radiometer (Haslam et al. 1974; Predmore et al. 1985), and, more recently, radiometers for observations of the Cosmic Microwave Background (e.g. WMAP; Jarosik et al. 2003). Analysis and laboratory tests show that this method will work very well for spectroscopy as well (Harris 2005). Correlation radiometry with the WASP2 analog lag correlators (Harris and Zmuidzinas 2001) has several practical advantages past the essential characteristic of excellent stability. First, a correlation receiver's two beams double the observing time efficiency compared with a conventional single-pixel receiver. Next, the two beams need only one cross-correlating analog lag spectrometer for a dual-beam receiving system, a significant savings in cost and complexity. Finally, analog correlators do not have the quantization noise penalty that can cost digital systems up to a factor of ~ 1.2 in signal to noise ratio.

Correlation detection is very stable because it makes an instantaneous differential power measurement. This greatly suppresses nonideal noise terms compared with conventional total power measurements. Consider first a total power radiometer with gain G, input source voltage v_{sou}, and system noise voltage v_n. Its detector output voltage v_{out} is proportional to $G\langle v^2_{detector}\rangle$, or $v_{out} \propto G\left(\langle v^2_{sou}\rangle + \langle v^2_n\rangle\right)$, plus a cross term that averages away with time as $1/\sqrt{B\tau}$. Spatial chopping and differencing between between source and reference positions on the sky largely eliminates the relatively large noise signal $\langle v^2_n\rangle$, but even tiny fluctuations in system gain G or noise power at the chop frequency can produce signals much larger than the weak source signal, $\delta\left(G\langle v^2_n\rangle\right) \gg \langle v^2_s\rangle$.

Cross-correlating radiometers have a hybrid circuit that combines voltages from the source and reference positions, v_s and v_r, with different but known phase shifts before amplification (Fig. 4). Cross-correlating the signals from the two amplifiers with the proper phase extracts the power difference between the source and reference positions, $v_{out} \propto G(\langle v^2_{sou}\rangle - \langle v^2_{ref}\rangle)$. Uncorrelated terms, including those from amplifier gain fluctuations, average away with time as $1/\sqrt{B\tau}$. Gain fluctuations have no large noise term to amplify, greatly reducing the excess noise across the spectrum. A full analysis (Harris 2005) shows that amplitude and phase imbalance reduce the signal but do not add correlated noise terms to the output.

Mathematics aside, a simple way to understand the technique is as a complement to the two-element spatial interferometer, where the correlated signal from two different antennas and receivers contains only information on the signal in common: that of the source. A single-dish correlation radiometer arranges the signal paths with as much commonality as possible; the only signals that are

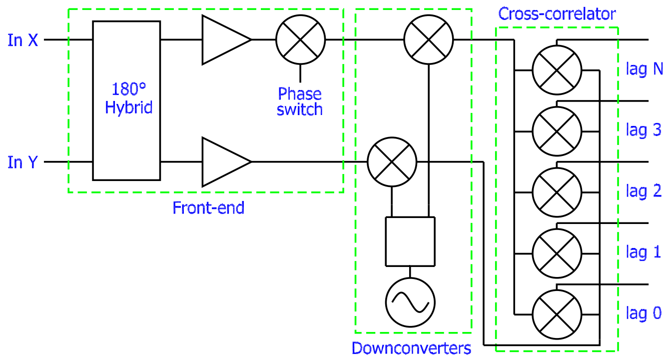

Figure 4. Top-level block diagram of the *Zpectrometer* system showing the Ka-band front-end, channelizing downconverter, and cross-correlator. See Fig. 5 for more detail on the correlator.

separate are the two from the signal and reference positions in the focal plane. The result, rather than the interferometer's detection of *correlated* signal in the aperture plane, is the difference of the *uncorrelated* power between two points in the focal plane.

3.2. Zpectrometer Hardware

Figure 4 is a top-level overview of the spectrometer system. NRAO is commissioning the Ka-band (26.5–40 GHz) correlation radiometer that we will use for the spectrometer's front-end. This radiometer was designed with an architecture similar to WMAP (Jarosik et al. 2003) for sensitive radio continuum measurements. After downconversion within the front-end into the 4–18 GHz band, an IF processor splits the signal into four 4–8 GHz band inputs for the cross-correlating spectrometers. A modest number of sub-bands allows compensation for slow changes in receiver and transmission system band flatness without introducing too many edge effects. Eight WASP2 analog lag correlation spectrometers (Harris and Zmuidzinas 2001), each with 3.7 GHz bandwidth and 128 lags produce the spectrum of the receiver band.

An analog lag correlator uses analog delays and multiplication to estimate the cross-correlation function $R_{XY}(\tau)$ as a function of lag τ:

$$R_{XY}(\tau) = \lim_{T\to\infty} \frac{1}{2T} \int_{-T}^{T} v_X(t) \cdot v_Y(t+\tau)\,\mathrm{d}t\ . \tag{1}$$

A Fourier transform of the cross-correlation function yields the power density cross-spectrum, which for the *Zpectrometer* is the power difference between the source and reference positions.

Figure 5 is a schematic diagram showing the correlator circuit board layout. The boards carry transmission lines that provide the time delays τ between multipliers, transistor multipliers that form the product of the two input voltages $v_A(t)$ and $v_B(t+\tau)$, and low-frequency electronics to integrate the multiplier output to provide the time average. Multiplier spacing sets the spectrometer's maximum bandwidth through the Nyquist theorem; increasing the total lag

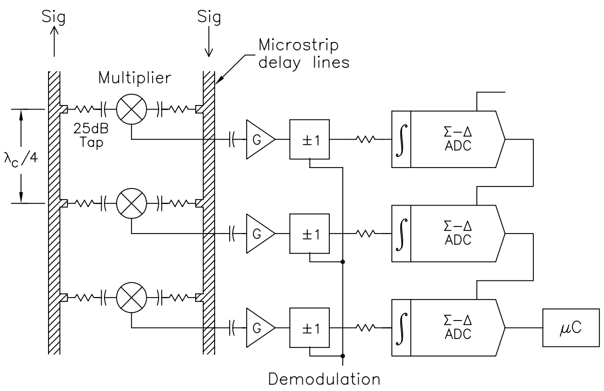

Figure 5. Schematic view showing a section of the "ladder" of multipliers within WASP2 and the low-frequency signal processing electronics. Sections of microstripline transmission line provide propagation-time delays between fast transistor multipliers.

time by adding multipliers to the ladder provides proportionally higher spectral resolution. The analog multipliers are commercial monolithic microwave integrated circuit (MMIC) transistor mixers with fast transistors in the same classical Gilbert multiplier core circuit (Gilbert 1968) that is in audio-frequency multiplier chips. Direct multiplication at the signal frequency means that only the low-frequency product term is digitized, a considerable saving in complexity and power dissipation.

Stability is a paramount concern for extragalactic spectrometers. WASP2's electronics have proved suitable for long integration times. Offset drift is usually the dominant problem for analog systems, but is largely removed by the layers of internal phase switching within WASP2. Allan variance characterization of spectrometer stability shows white noise to times beyond 100 seconds for the high lags, which should be representative of all lags in cross-correlation mode. This timescale is well within the timescale for efficient beam exchange at the GBT.

3.3. Correlator configurations

Table 1 shows a number of possible correlator configurations that could cover different bands in different ways. The *Zpectrometer* correlator contains a total of 1024 lags that may be distributed in 128 lag subsets, each subset covering 3.5 GHz. The initial configuration for Ka-band, shown in bold, is 4 subbands of 256 lags. This covers as much bandwidth as possible and requires no tuning between the front-end and correlator package.

In this initial configuration, the *Zpectrometer* will cover the entire Ka-band with spectral resolution of about 150 km s^{-1}. This is sufficient for characterizing the dynamics of high-redshift galaxies. Hainline et al. (2004) summarize 27 published CO detections from $z > 1.4$ galaxies, finding a median FWHM velocity width of 380 km s^{-1} and a range from 170 to 840 km s^{-1}, values confirmed by later observations (Greve et al. 2005; Tacconi et al. 2006). WASP2 configured for 256 lags matches this very well. Figure 6a is a 128-lag WASP2 spectrum of the 230 GHz CO J = 2–1 line from the starburst nuclear ring in the Seyfert

Bandwidth GHz	Resolution MHz	Polarizations	Number of subbands	Lags per subband
28	32.8	1	8	128
14	**16.4**	**1**	**4**	**256**
7	8.2	1	2	512
7	16.4	2	2	256
3.5	16.4	2	1	512

Table 1. Some possible correlator configurations. Switching between configurations requires some modification of the downconversion electronics and some internal cables. Boldface denotes the *Zpectrometer*'s initial configuration.

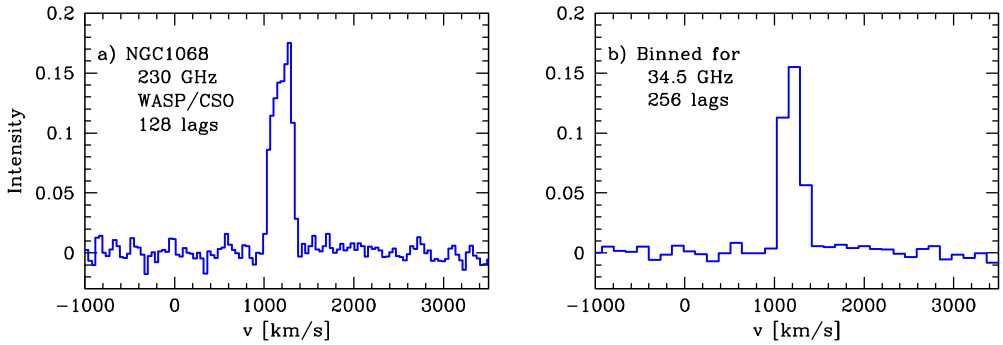

Figure 6. Measured and simulated signals from the WASP spectrometers. a) Measured CO $J = 2$–1 line at the CSO with 128 lag autocorrelator mode; b) Same spectrum binned to show resolution at 34.5 GHz with 256 lags.

galaxy NGC1068, which has a width of about 300 km s^{-1}. This spectrum was one of four contiguous WASP2 sub-bands obtained with the wideband 200–300 GHz receiver at the Caltech Submillimeter Observatory in August 2003. No corrections have been applied to the spectral baseline. Figure 6b is the same spectrum binned to simulate an observation of the same source in the CO $J =$ 1–0 line at $z = 2.3$ (34.5 GHz) with a 256-lag WASP2.

Connecting the *Zpectrometer* back-end hardware to other GBT front-ends can provide wideband spectroscopy at all values of z. Obvious extensions are to reconfigure for autocorrelation with the K-band (18-26.5 GHz) or Q-band (40-50 GHz) front-ends. These are conventional total-power receivers, so the advantages of correlation techniques would be lost. An additional downconverter system and minor internal recabling would cover entire 28 GHz W-band (3 mm) HEMT amplifier bands with 33 MHz resolution; the GBT W-band front-ends will have correlation architectures.

3.4. Data acquisition and analysis

Each pair of correlators shares an internal microcomputer that handles all real-time data acquisition and accumulates the correlator digital output for some integration time. An Ethernet connection takes the lag data from the microcomputer to one of the GBT's computers to a reduction pipeline that converts to the spectral domain, calibrates amplitude and frequency scales, and writes a calibrated file for further analysis.

Finding lines within a spectrum of over 40% bandwidth is unlike previous radio spectroscopy. We are developing analysis tools that use the time series as well as the average spectrum to estimate fluctuations for each spectral channel; see Zonak, Baker, and Harris in this *Proceedings* for further details.

4. Timeline and operation

Fabrication began in March 2005 with a target for first tests in the winter of 2006/2007 and science observations the following winter. The *Zpectrometer* is a collaboration between the University of Maryland (UMD) and the National Radio Astronomy Observatory (NRAO). Following NRAO's policy on external instrumentation, this system will be open for community proposals in a shared-risk mode after early commissioning. The instrument will transition to a facility-mode instrument after the 2008/2009 winter.

Acknowledgments. The *Zpectrometer* is being constructed with National Science Foundation (NSF) grant AST-0503946 to the University of Maryland. The NRAO is operated for the NSF by Associated Universities, Inc., under a cooperative agreement.

References

C. M. Bradford, T. Nikola, G. J. Stacey, A. D. Bolatto, J. M. Jackson, M. L. Savage, J. A. Davidson, and S. J. Higdon. ApJ, 586:891–901, 2003.
D. Downes and P. M. Solomon. ApJ, 507:615–654, 1998.
Y. Gao and P. M. Solomon. ApJ, 606:271–290, 2004.
R. Genzel, A.J. Baker, R.J. Ivison et al. astro-ph/0403183, 2004.
B. Gilbert. *IEEE J. Solid-State Circuits*, 3:365–373, 1968.
T. R. Greve et al. MNRAS, 359:1165–1183, 2005.
L. J. Hainline, N. Z. Scoville, M. S. Yun, D. W. Hawkins, D. T. Frayer, and K. G. Isaak. ApJ, 609:61–68, 2004.
A. I. Harris. *Review of Scientific Instruments*, 76:4503–+, 2005.
A. I. Harris, J. Stutzki, U. U. Graf, A. P. G. Russell, R. Genzel, and R. E. Hills. ApJ, 382:L75–L79, 1991.
A. I. Harris and J. Zmuidzinas. *Review of Scientific Instruments*, 72:1531–1538, 2001.
C.G.T. Haslam, W.E. Wilson, D.A. Graham, and G.C. Hunt. *Astron. Astrophys. Suppl.*, 13:359–394, 1974.
J. R. Houck et al. ApJ, 622:L105–L108, 2005.
N. Jarosik et al. *Astrophys. J. Suppl. Ser.*, 145:413–436, 2003.
M. L. Luhman, S. Satyapal, J. Fischer, M. G. Wolfire, E. Sturm, C. C. Dudley, D. Lutz, and R. Genzel. ApJ, 594:758–775, 2003.
R. Q. Mao, C. Henkel, A. Schulz, M. Zielinsky, R. Mauersberger, H. Störzer, T. L. Wilson, and P. Gensheimer. A&A, 358:433–450, 2000.
C.R. Predmore, N.R. Erickson, G.R. Huguenin, and P.F. Goldsmith. *IEEE Trans. Microwave Theory Tech.*, MTT-33:44–51, 1985.
M. Reuland, H. Röttgering, W. van Breugel, and C. De Breuck. MNRAS, 353:377–390, 2004.
N. Z. Scoville, M. S. Yun, and P. M. Bryant. ApJ, 484:702–+, 1997.
L. J. Tacconi, R. Neri, S. C. Chapman, R. Genzel, I. Smail, R. J. Ivison, F. Bertoldi, A. Blain, P. Cox, T. Greve, and A. Omont. ApJ, 640:228–240, March 2006.

J. S. Ward, J. Zmuidzinas, A. I. Harris, and K. G. Isaak. ApJ, 587:171–185, 2003.
L. Yan et al. ApJ, 628:604–610, 2005.